AVOA attribute analysis and cross-plotting for time-lapse monitoring of stress and saturation changes: Application to the Teal South 4D-4C dataset

Stephen A. Hall and Colin MacBeth.*

Department of Petroleum Engineering, Heriot-Watt University, Edinburgh, UK.

Summary

AVO analysis and cross-plotting have become established techniques for risk reduction in hydrocarbon exploration and production. More recently these concepts have been applied to repeat seismic surveys to assess production related changes in hydrocarbon reservoirs. Here these methods are further extended to provide amplitude variation with offset and azimuth (AVOA) attributes and cross-plotting tools for monitoring changes in reservoir stress and fluid properties using 4D-4C data. New theory for interpretation of AVOA cross-plots and definition of background trends is presented in terms of anisotropy and fracture parameters These equations allow analysis of time-lapse variations in stress or saturation with the possibility of distinguishing changes in matrix properties from those associated with fractures or low aspect-ratio porosity. The insight gained is used to interpret AVOA data from the Teal South 4D-4C experiment.

Introduction

Aligned, low aspect-ratio porosity and fractures strongly influence permeability so are critical factors in a reservoir's production but they are also are highly sensitive to perturbations in the local and regional stress fields. However characterisation and monitoring of such low aspect-ratio constituents of a reservoir is beyond the resolution of standard seismic techniques. If the low aspect-ratio porosity in a reservoir is aligned giving rise to seismic anisotropy it may be mapped spatially and temporally using AVOA analysis of repeat 3D surveys (Hall and MacBeth 2001). AVOA analysis has significant sensitivity to aligned fractures or low aspect-ratio porosity and to their fluid-fill/saturation (e.g., Hall and Kendall 2000). Therefore observations of AVOA can be used to assess small changes in this aligned porosity and possibly distinguish fluid movements controlled along these permeability pathways from saturation changes in the rock matrix. This paper first provides background on AVO in anisotropic media before outlining the basis of AVO crossplotting which leads to the development of tools for AVOA attribute analysis. A real data example from the Teal South field is presented and interpreted using the derived equations to demonstrate the potential for enhanced understanding of reservoir saturation and stress changes.

Time-lapse AVOA analysis in the Teal South 4D-4C data

The Teal South 4D-4C experiment in the Gulf of Mexico, managed by the Energy Research Clearing House in Houston, involved two phases of 3D-OBC acquisition with a 2-year interval as outlined by Ebrom et al. (1998). The reservoirs of interest are turbidite sands distributed between 4000' and 8000'. This work concentrates on the 4500' sand where a clear time-lapse response between the legacy towed-streamer and the Phase I OBC datasets was observed. Conventional processing and analysis of the Phase I and II OBC surveys revealed an insignificant time-lapse signature. In this period, between the two OBC acquisition phases, the reservoir changes detected at the well involved: a pressure decrease from 19.5 MPa to 15.1Mpa, with the rock stress being 36MPa; a saturation (Sg:So:Sw) change of 0.00:0.70:0.30 to 0.05:0.65:0.3; a change in fluid properties from a density of 797kgm^{-3} and Vp of 1240ms^{-1} to values of 761kgm^{-3} and 1140ms^{-1} respectively. Thus only small changes in the reservoir occurred and enhanced monitoring techniques are necessary. Hall and MacBeth (2001) presented results of time-lapse AVOA analysis at Teal South using the approach of Hall et al. (2000). This work provided maps of AVO anisotropy for a small area of the producing interval showing spatial variations that were greater than those predicted from the reservoir changes at the well. This may be related to the bulk saturation changes that are expected in this region as it lies near the oil water contact (OWC). Additionally, since the reservoir was initially over-pressured, some degree of compaction is expected that may lead to changes in local stress distributions. Analysis of these results is presented here using the new 4D AVOA attribute analysis techniques to further constrain the reservoir changes and to attempt to separate matrix and fracture effects.

AVO in azimuthally anisotropic media

At a boundary between two isotropic half-spaces the reflectivity varies as a function of incident phase angle, i (i.e., AVO). This is commonly approximated for the purposes of data analysis, e.g., for the P-P reflection amplitude,

$$R_{pp}(i) = A + B\sin^2 i + C\sin^2 i\tan^2 i. \qquad (1)$$

The terms A, B and C are defined, for example, by Chapman (1976), as,

$$A = \frac{1}{2}\frac{\Delta Z}{\overline{Z}}, B = \frac{1}{2}\left[\frac{\Delta\alpha}{\overline{\alpha}} - \left(\frac{2\overline{\beta}}{\overline{\alpha}}\right)^2\frac{\Delta G}{\overline{G}}\right], C = \frac{1}{2}\frac{\Delta\alpha}{\overline{\alpha}}. \qquad (2)$$

Here $Z = \rho\alpha$ is the P-wave impedance and $G = \rho\beta^2$ is the shear modulus where α, β and ρ are, respectively, the P-wave velocity, the shear-wave velocity and the density. The symbol Δ indicates differential values, for example $\Delta\alpha = \alpha_2 - \alpha_1$, and the over-scored terms are the average

values, e.g. $\overline{\alpha} = (\alpha_2 + \alpha_1)/2$, where the subscripts, 1 and 2, indicate the properties of the upper and lower bounding media respectively.

Alignment sub-seismic scale fracturing or low aspect-ratio porosity can produce seismic anisotropy leading to measurable directional differences in travel-times and reflectivity. Vertically aligned fractures will produce azimuthal anisotropy (the simplest case being horizontal transverse isotropy, HTI) such that reflectivity of an interface depends on azimuth as well as offset. Thus equation 1 must be extended, as by Rüger (1998) and Vavryčuk and Pšenčík (1998), to describe the AVOA. These works show that in HTI media AVO varies azimuthally as functions of $\cos 2\phi$ and $\cos 4\phi$ (for more complex symmetries than HTI there maybe additional, higher order, terms in $\cos\phi$). At near offsets the $\cos 2\phi$ component will dominate for many cases (e.g., Hall and Kendall, 2000) so the AVOA equations can often be simplified using just terms in $\cos 2\phi$ (although this should be verified by data observations). Thus the gradient term in equation 1, as a function of the azimuth from the fracture normal direction, ϕ, becomes,

$$B' = \frac{1}{2}\left[\frac{\Delta\alpha}{\overline{\alpha}} - \left(\frac{2\overline{\beta}}{\overline{\alpha}}\right)^2 \frac{\Delta G}{\overline{G}}\right] + \frac{1}{2}\left[\Delta\delta^{(v)} - 2\left(\frac{2\overline{\beta}}{\overline{\alpha}}\right)^2 \Delta\gamma^{(v)}\right]\cos^2\phi, \tag{3}$$

(adapted from Rüger, 1998). The gradient is now a function of the contrasts in velocities plus the azimuthal anisotropy parameters across the reflecting interface. The long offset term, C in equation 1, will be a function of higher order cosine terms but is neglected here since only near-offsets are considered at present and a $\cos 2\phi$ azimuthal trend is assumed. The values α and β are now the vertical P-wave velocity and the velocity of the shear-wave propagating in the vertical plane and polarised parallel to the fractures. $\epsilon^{(v)}$ and $\delta^{(v)}$ are the Thomsen-like parameters used to study HTI media (e.g., Rüger 1998) defined in terms of the elasticities, C_{ij}, as,

$$\gamma^{(v)} = \frac{C_{66} - C_{44}}{2C_{44}}, \qquad \delta^{(v)} = \frac{(C_{13} + C_{66})^2 - (C_{33} - C_{66})^2}{2C_{33}(C_{33} - C_{66})}. \tag{4}$$

AVO cross-plotting and background trends in azimuthally anisotropic media

Variations in the physical properties of the rocks bounding an interface mean that for individual reflectors the AVO will vary spatially. However, a good correlation often exists between the variations of each of these properties such that when the AVO gradient, B, is plotted against the intercept, A, an underlying "background" trend is observed (e.g., Smith and Gidlow, 1987). The actual AVO attributes will plot about this line in A-B space as an elliptical cloud. Based on the data and assumptions about the interdependence α, β and ρ the Background Trends (BTs) can be determined. Deviations from the BT can thus be assessed to define anomalies that may, for example, relate to hydrocarbon rich zones. To achieve this analysis Castagna et al. (1998) define the AVO intercept and gradient parameters in equation 1 as,

$$A = \frac{1}{2}\left(\frac{\Delta\alpha}{\overline{\alpha}} + \frac{\Delta\rho}{\overline{\rho}}\right), \qquad B = \frac{1}{2}\left[\frac{\Delta\alpha}{\overline{\alpha}} - \left(\frac{2\overline{\beta}}{\overline{\alpha}}\right)^2 \left(2\left(\frac{\Delta\beta}{\overline{\beta}}\right) + \frac{\Delta\rho}{\overline{\rho}}\right)\right]. \tag{5}$$

Thus using Gardner's relationship (Gardner et al., 1974),

$$\left(\frac{\Delta\rho}{\overline{\rho}}\right) \approx g\left(\frac{\Delta\alpha}{\overline{\alpha}}\right), \tag{6}$$

and the general relationship between α and β (e.g., Castagna et al., 1998),

$$\alpha = m\beta + c, \tag{7}$$

the background A-B trend may be defined from equation 5 (Castagna et al. 1998) as,

$$B = \frac{A}{1-g}\left\{1 - \left(\frac{2\overline{\beta}}{\overline{\alpha}}\right)^2 \left[\frac{2}{m} + g\left(\frac{2\overline{\beta}}{\overline{\alpha}}\right)\right]\right\}. \tag{8}$$

In the presence of aligned fractures/porosity the AVO gradient will vary azimuthally and two main axes of anisotropy will exist. Analysis of the AVO attributes along these two axes will provide insight into the background matrix properties and the nature of the aligned porosity. For the simple case of an HTI medium (e.g., a single set of aligned fractures) the AVO parallel to the fracturing will be largely unaffected by the fracture properties (equation 3). Thus along this direction the background trend, $BT_{\parallel}$, on the A-B crossplot will be defined by equation 8. However along the axis perpendicular to this, i.e., the fracture normal direction, the AVO gradient will be perturbed from the isotropic background trend by some factor determined by the anisotropy contrasts, $\Delta\gamma^{(v)}$ and $\Delta\delta^{(v)}$. By comparison of equations 2, 3 and 5 the background trend along this axis, $BT_{\perp}$, can be defined as,

$$B_{\perp} = \frac{A}{1-g}\left\{1 - \left(\frac{2\overline{\beta}}{\overline{\alpha}}\right)^2 \left[\frac{2}{m} + g\left(\frac{2\overline{\beta}}{\overline{\alpha}}\right)\right]\right\} + \frac{1}{2}\left\{\Delta\delta^{(v)} - 8\left(\frac{\overline{\beta}}{\overline{\alpha}}\right)^2 \Delta\gamma^{(v)}\right\}. \tag{9}$$

If the anisotropy is induced by aligned fractures $\gamma^{(v)}$ and $\delta^{(v)}$ may be cast in terms of the non-dimensional fracture parameters, e_N and e_T,

$$\gamma^{(v)} = -\frac{e_T}{2}, \qquad \delta^{(v)} = -2\left(\frac{\beta}{\alpha}\right)^2 \left[\left(1 - 2\left(\frac{\beta}{\alpha}\right)^2\right) e_N + e_T\right]. \tag{10}$$

Thus $BT_\perp$ may now be determined in terms of fracture properties (for an isotropic overburden and assuming that $\frac{\beta}{\alpha} \approx \frac{\overline{\beta}}{\overline{\alpha}}$) as,

$$B_\perp = \frac{A}{1-g}\left\{1-\left(\frac{2\overline{\beta}}{\overline{\alpha}}\right)^2\left[\frac{2}{m}+g\left(\frac{2\overline{\beta}}{\overline{\alpha}}\right)\right]\right\} + 2\left(\frac{\overline{\beta}}{\overline{\alpha}}\right)^2\left[e_T-\left(1-2\left(\frac{\overline{\beta}}{\overline{\alpha}}\right)^2\right)e_N\right]. \quad (11)$$

The parameters e_N and e_T are defined by Schoenberg and Sayers (1995) from the additional fracture compliances, Z_N and Z_T, and the Lamé parameters of the background rock matrix, λ_b and μ_b, such that,

$$e_N = \frac{Z_N(\lambda_b+2\mu_b)}{1+Z_N(\lambda_b+2\mu_b)}, \qquad e_T = \frac{Z_T\mu_b}{1+Z_T\mu_b}. \quad (12)$$

These terms describe a range of fracture scenarios that can be described using different definitions of Z_N and Z_T, e.g., for penny-shaped voids (Hall and Kendall, 2000),

$$Z_N = \frac{4\eta_c}{3\mu_b}\frac{1}{1-\left(\frac{\beta}{\alpha}\right)^2}\frac{1}{1+K}, \qquad Z_T = \frac{16\eta_c}{3\mu_b}\frac{1}{3-2\left(\frac{\beta}{\alpha}\right)^2}, \quad (13)$$

where $K = \frac{\kappa_f}{\pi d \mu_b}\frac{1}{1-\left(\frac{\beta}{\alpha}\right)^2}$. Thus $B_\perp$ can be directly related to the properties of both the rock matrix and fractures. Changes in the matrix velocity ratio, β/α, the fluid bulk modulus, κ_f, the porosity aspect ratio, d, and the crack density, η_c, will all produce a dc-shift in $BT_\perp$ relative to $BT_\parallel$. Altering β/α, κ_f or d can also cause the anisotropy to go from a positive to a negative azimuthal variation as the ratio of the e_N and e_T parts of equation 11 will be affected. Equations 8 and 11 show that $\overline{\beta}/\overline{\alpha}$ influences both BTs, by changing their gradients, so matrix saturation variations have a different effect to changes in the fracture parameters.

Teal South data example

Figure 1 shows A-B AVOA cross-plots for a small area of the phase I and II OBC surveys at Teal South from the results of Hall and MacBeth (2001). The two anisotropy axes are plotted; λ_1, the most-positive AVO gradient, in green and λ_2 in red. The reservoir sandstone ($Vp = 2210ms^{-1}$ and $\rho = 2030kgm^{-3}$) is overlain by shale ($Vp = 2740ms^{-1}$ and $\rho = 2300kgm^{-3}$) providing a negative impedance contrast at the interface. These properties are derived from limited log data and lead to $g \approx 0.6$ (see equation 6). Kelly (2000) suggests standard values for the Gulf of Mexico for m and c of about 1.16 and 1160 respectively. However the data being considered here suggest a value of 1.11 for m may be more appropriate in this case. Figures 1(i)b and 1(ii)b show estimated background trends determined using these parameters and an HTI fracture model with η_c=0.1 and d=0.001. Ellipses are also drawn to highlight the main data trends. The yellow, dotted ellipse in Figure 1(ii)b is a possible anomalous non-parallel data trend that incorporates both λ_1 and λ_2 data; this is discussed further in the following section.

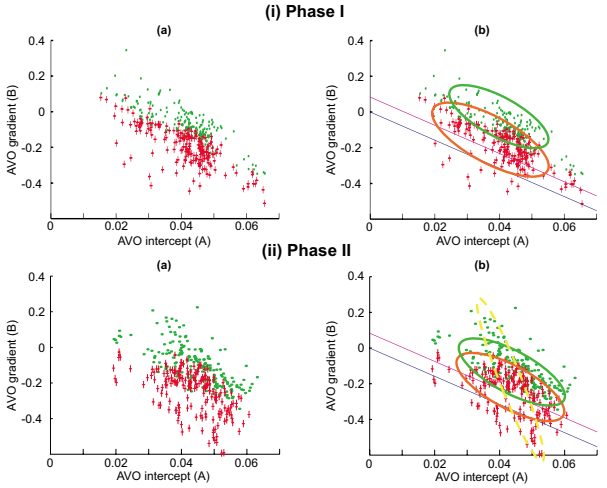

Figure 1 A-B AVOA cross-plots for a small area of the (i) phase I and (ii) phase II OBC surveys at Teal South from the results Hall and MacBeth (2001). Figures (a) show the A-B data and figures (b) show interpreted ellipses indicating the trends in the data plus background trends predicted using the parameters outlined in the text. The two anisotropy axes are plotted with λ_1, the most-positive AVO gradient, in green and λ_2 in red.

The Phase I crossplot shows two clear trends, corresponding to the two anisotropy directions, which align roughly with the predicted background trends. The separation of the data trends is approximately the same as in the model. Figure 1b shows the AVOA crossplot for the Phase II Teal South data over the same area as Figure 1a plus the same predicted BTs. The scatter in the Phase II cross-plot is much greater than in Phase I. However a reasonable λ_2 trend can be defined that is approximately consistent with Phase I. A second, parallel trend for λ_1 exists but is less well defined. This trend is consistent with the Phase I data but has a smaller offset from the λ_2 trend indicating a general reduction in the anisotropy from Phase I to II. For this interpretation calibration of the crossplots is necessary for each phase and between the two phases utilising data away from the producing zone (e.g., Kelly, 2000).

Discussion

The analytical equations provided for the BTs indicate that HTI anisotropy will provide two discrete, but parallel, background trends on the A-B crossplots. This appears to be observed in the data from Phase I and, less distinctly, in Phase II. Such a situation could exist only where the stress distribution is largely dominated by some long wavelength (regional) trend and the saturation does not vary greatly. If the stress-state varies, the fracture parameters (e.g., aspect ratio) and thus $BT_\perp$ are affected

giving a change in the separation of the two BTs and greater scatter of the fracture normal AVO from the $BT_\perp$ trend. $B_\parallel$ should remain consistent and close to $BT_\parallel$, being dependent solely on the variations in the rock matrix. Thus a distinct $BT_\parallel$ should generally be observed but a clear $BT_\perp$ will not necessarily be observed. The effects of varying matrix saturation differ from stress perturbations in that only the separation of the trends will be affected by stress whereas for a saturation change the gradients of both BTs will also be altered, though they will remain parallel. Changes in the saturation of the low aspect-ratio porosity, as opposed to that of the equant matrix porosity, will lead to a change in the separation of the two BTs but not their gradients. Thus matrix saturation and fracture effects could possibly be distinguished but separation of fracture saturation and stress effects can not.

The increased scatter in the Phase II crossplot could indicate that saturation and stress in the area become more heterogeneous, consistent with the movement of the OWC. However the reduced separation of the λ_1 and λ_2 trends in Phase II with little change in the gradients over time suggests a change in fracture properties as opposed to a general saturation change across the area. The third trend identified on the Phase II cross-plot, highlighted by the yellow ellipse, cross-cuts the main trends and includes data from both λ_1 and λ_2. Such a trend can only be explained if the changes in the anisotropy are linked to changes in A resulting in non-parallel BTs and crossing trends. This is related to the change from a positive to negative azimuthal variation, due to variations in α/β, κ_f or d but not η_c, suggested by Hall and Kendall (2000) and MacBeth (2000). The λ_2 trend in general shows less scatter than λ_1 and has a greater consistency from phase I to II. $B_\parallel$ is less dependent on fluid and stress changes than $B_\perp$ so should be more consistent spatially and over time. Therefore it is suggested that the general fracture strike is likely to be aligned with λ_2. Hall et al. (2000) and Hall and Kendall (2000) highlight that the determination of which axis, λ_1 or λ_2, is the fracture strike direction is not always straight-forward but these cross-plots appear to provide additional insight that could reduce this ambiguity.

Conclusion

This work has provided new equations to allow AVOA attribute analysis and crossplotting that could lead to improved insight into the nature of reservoir anisotropy and provide the potential to monitor small production-related changes in reservoir saturation and stress-state. Furthermore, this approach may allow changes in the matrix to be distinguished from changes in the fracture properties. However separating fracture related stress and saturation changes may not be possible. The equations provided are for HTI media but more complex anisotropies, e.g., including layering or additional fracture alignments, may be addressed with additional anisotropy terms in either of the BT equations (e.g., Chen et al., 1999 for layered media). An initial qualitative analysis has been carried out in the producing zone of the 4500' sand at Teal South showing a time-lapse change in the anisotropy characteristics that are interpreted as general changes in fracture properties and localised saturation changes. Future converted wave attribute analysis and cross-plotting techniques will provide additional insight that could allow further separation of stress and saturation or matrix and fracture changes. This work ultimately leads to a more quantitative assessment of time-lapse processes permitting improved constraint on the reservoir simulation.

Acknowledgements

We would like to thank the Energy Research Clearing House (ERCH), in particular Roger Entralgo, and 4D-4C consortium sponsors for the Teal South data set. We would also like to acknowledge the support of the Edinburgh Time-lapse Project sponsors: BP, Concept Systems, Enterprise Oil, Fairfield Industries, Landmark, Schlumberger, Shell and TotalFinaElf.

References

Castagna, J. P., Swan, H. W. and Foster, D. J., 1998, Framework for AVO gradient and intercept interpretation: Geophysics, 63, no. 03, 948-956.

Chen, H., Ramos, A., Brown, R. and Castagna, J., 1999, Three-parameter AVO crossplotting in anisotropic media: 69th Mtg., Soc. Explor. Geophys., Expanded abstracts, 73-76.

Ebrom, D., Krail, P., Ridyard, D. and Scott, L., 1998, 4-C/4-D at Teal South: The Leading Edge, 17, no. 10, 1450-1453.

Gardner, G. H. F., Gardner, L. W. and Gregory, A. R., 1974, Formation velocity and density - The diagnostic basics for stratigraphic traps: Geophysics, 39, no. 06, 770-780.

Hall, S.A. and Kendall, J-M., 2000, Constraining the interpretation of AVOA for fracture characterisation, Anisotropy 2000: Fractures, converted waves and case studies, Proceedings of the Ninth International Workshop on Seismic Anisotropy (9IWSA).

Hall, S.A. and MacBeth, C.D., 2000, Multicomponent time-lapse AVOA analysis at Teal South, SEG/EAGE Summer Research Workshop: Recent advances in shear wave technology for reservoir characterisation: A new beginning? Soc. Explor. Geophys, October 1-6, 2000, Boise, Idaho

Hall, S.A. and MacBeth, C.D., 2001, 4D-4C AVOA at Teal South, 63rd, Mtg., Eur. Assoc. Explor. Geophys., Expanded Abstracts.

Hall, S.A., Barkved, O.I., Mueller, M.C. and Kendall, J-M., 2000, An approach for P-wave AVOA in 3D-OBC data, 62nd Mtg., Eur. Assoc. Explor. Geophys., Expanded Abstracts, Paper: C-09.

Kelly, M., 2000, The interpretation of P-P AVO crossplots: 70th Internat. Mtg., Soc. Explor. Geophys., Expanded abstracts.

MacBeth, C.D., 2000, Using P-wave data to distinguish between gas from water in fractures, Anisotropy 2000: Fractures, converted waves and case studies, Proceedings of the Ninth International Workshop on Seismic Anisotropy (9IWSA).

Rüger, A., 1998, Variation of P-wave reflectivity with offset and azimuth in anisotropic media: Geophysics, 63, 935-947.

Schoenberg, M. and Sayers, C. M., 1995, Seismic anisotropy of fractured rock: Geophysics, 60, no. 01, 204-211.

Smith, G.C. and Gidlow, P.M., 1987, Weighted stacking for rock property estimation and detection of gas: Geophysical Prospecting, 35, 993-1014.

Vavryčuk, V. and Pšenčík, I., 1998, PP-wave reflection coefficients in weakly anisotropic elastic media: Geophysics, 63, no. 06, 2129-2141.